Progress Report

NSTIF

E82-101 36

CR-168521

on

(E82-10136) COMPATIBILITY STUDY OF THE MAGSAT DATA AND AEROMAGNETIC DATA Progress Report (North Carolina State Univ.) 15 p HC A02/MF A01 CSCL 05B

N82-21663

Unclas
G3/43 00136

Compatibility Study of the MAGSAT Data and Aeromagnetic Data

NAS5-26157

Submitted by

I. J. Won
Department of Marine, Earth and Atmospheric Sciences
North Carolina State University
Raleigh, North Carolina 27650

August, 1981

Summary of Report

This progress report contains the results of (1) analysis of the fine attitude MAGSAT data from November 1 through December 22, 1979 covering the continental U.S., (2) analysis of the Project MAGNET U.S. aeromagnetic data in terms of its compatibility with the corresponding MAGSAT data, and finally, (3) analysis of MAGSAT data in the Pacific region and comparison with satellite gravity data.

(1) Analysis of MAGSAT Data in the U.S. Region

The available fine attitude data paths over the continental U.S. during the period are shown in Figure 1. The area, bounded by latitudes 24N-52N and longitudes 230E-295E, contains a total of 306 paths, counting the north-bound paths and the south-bound paths separately.

The paths contain a total of some 28,000 scalar magnetic data. Screening obviously bad data, based upon a criteria of anomaly amplitude, removed about 3,400 data points. The resultant map, contoured at a two-gamma interval, is shown in Figure 2.

One notices immediately that there are numerous narrow north-south trending anomalies. These anomalies are believed to be caused by possible orbital offset errors, i.e., each path may have a different static bias, drift rate, etc. Our first attempt was to remove only the static bias by minimizing the rms difference between the data along each individual path and the predicted reference field data. This removes a certain constant from each orbital data set. The resultant map is shown in Figure 3. The standard deviation of the static bias for the entire 306 paths is computed to be 5.9 gammas. We note noticeable improvements (in terms of the continuity of anomalies) particularly in the middle of the U.S. continent. The major anomalous feature in the southern U.S. is now reasonably continuous and discernible.

To further investigate the possible orbit-induced errors, we removed, in a least-squares sense, a first-order polynomial from each path. This removes both the static bias and the drift. The outcome is shown on Figure 4. Most of the N-S trending narrow anomalies now have disappeared. Assuming that this is an improvement over the previous maps, we may conclude that the MAGSAT data contain both the static bias and the drift errors which must be corrected on a path-by-path basis. The average slope for the 306 paths in this region is found to be 3.5×10^{-3} gammas/km with a standard deviation of 5.7×10^{-3} gamma/km, implying that the drift rates are more or less random among the paths. A further correction using a second-order polynomial for each path (Figure 5) did not change the result significantly and showed signs of over-correction indicated by some diminishing long wavelength anomalies. Based on these results we may conclude that the first-order correction is optimal and sufficient.

(2) Analysis of the MAGNET U.S. Aeromagnetic Data

The main objective of our original proposal pertains to the comparison of the MAGSAT data and the available aeromagnetic data in the eastern U.S. We have put considerable effort into preparing a large scale U.S. aeromagnetic map which can be upward-continued to the satellite altitude. Most of the state or local aeromagnetic maps, due to various reasons, cannot be easily patched up to make a large scale map.

For this reason, we acquired the entire MAGNET U.S. aeromagnetic survey data from the National Geophysical and Solar-Terrestrial Data Center (NGSTD) of NOAA. The data were collected during 1976 and 1977 at altitudes (AGL) of 500-700 m in non-mountainous terrain and 900-1,000 m in mountainous terrain. The MAGNET file contains some 650,000 measurements at approximately 100 m intervals along the flight path. Spacing between the N-S flight paths is about 1.1 degree in longitude. Since the data density along the path is much higher than the line spacing, we averaged over every 100 data points to reduce the total data amount to about 6,500. This gives approximately 0.1 degree sampling interval along the path. Figure 6 shows the total field contour map along with the flight paths.

A 13th order and degree reference field of GSFC (9/80-2) with the secular variation was removed from the MAGNET scalar data to produce a U.S. aeromagnetic anomaly map shown on Figure 7. The residual field thus obtained still contains considerably long wavelength anomalies, particularly in the northern latitudes. It is most likely due to insufficient removal of the non-crustal field. Other reference field models produce varying yet similar results.

In an effort to reduce further the remaining non-crustal field from the data, we removed a best-fitting low-order polynomial surface. Figure 8 shows an exemplary result after removing a third-order polynomial surface from the map of Figure 7. The map thus produced has a considerable resemblance to the MAGSAT anomaly map of Figure 5. Similarities are particularly noticeable along an arc connecting the Texas-Appalachian-Great Lakes-Montana region, where major magnetic highs occur in both the satellite and the aeromagnetic anomaly maps.

The resultant MAGNET anomaly map, which is believed to be the best large-scale representation of the region, is next upward-continued by 200 km (Figure 9) and by 300 km (Figure 10), respectively. The overall resemblance between the MAGNET and the MAGSAT data is still clearly noticeable throughout the region. We believe that this is the first direct proof that the MAGSAT data are compatible with the surface magnetic data on a large scale.

(3) Analysis of MAGSAT Data in the Pacific Region and Comparison with Satellite Gravity Data

To further study compatibility of the MAGSAT data and surface geophysical data we compiled the MAGSAT data in the Pacific region bounded by latitudes 35S-55N and longitudes 90E- 00E. The orbital paths of these data are shown in Figure 11. There are a total of 943 paths (counting the north-bound and the south-bound paths separately) having a total of some 240,000 data points during the period of November 1, 1979 through December 22, 1979.

After removing bad data and choosing every fifth data point we used a total of 46,510 points to produce a scalar anomaly map of the region shown on Figure 12. Again, we notice numerous N-S trending narrow anomalies which are considered to be caused by the orbital offset and drift errors. Figure 13 shows the resultant map after removing a best-fit first-order polynomial from each path. The average static bias is found to be -9.4 gammas with a standard deviation of 11.1 gammas while the average drift rate is 0.705×10^{-3} gammas/km with a standard deviation of 3.6×10^{-3} gammas/km. For both parameters, the large standard deviations imply that the static offsets and drifts are random among the orbital paths. Removing a best-fit second order polynomial from each path further smooths the data as shown on Figure 14. It appears that most of the possibly orbit-induced anomalies are suppressed in this map, which may be considered perhaps the best representation of the true anomaly map.

Unfortunately, there is no ground magentic anomaly map compiled for the area. Therefore, we attempted to compare the MAGSAT data with a gravity anomaly map derived from satellite-to-satellite tracking data using the GEOS-3 geodetic satellite (Marsh et al., 1981) shown on Figure 15. We notice some quantitative correlation between the two maps in such regions as the northern Pacific Ocean between latitudes 30N-40N and the neighborhood of the southeastern Asian islands. In order to further correlate these data, we derived a second vertical derivative map of the same data using an algorithm developed by Hildenbrand (1978). The resultant map is shown in Figure 16. The comparison is considered meaningful because the second vertical derivatives of gravity data generally emphasize the geological boundaries where the magnetic anomalies often become prominent. Neglecting the map boundaries having the edge effect of the continuation process, we notice generally good agreements between this map and the MAGSAT anomaly map of Figure 14. It is encouraging to note that correlations of the anomalies in the northern Pacific and the southeastern Asian islands to those of MAGSAT data have further improved.

Based on these results, we may tentatively conclude that the MAGSAT data do represent and are generally compatible with available surface geophysical data in the regional scales studied in this report.

References

Marsh, J.G., Marsh, B.D., Williamson, R.G., Wells, T.W., 1981, The gravity field in the central Pacific from satellite-to-satellite tracking, J. Geoph. Res., 86, B5, 3979-3997.

Hildenbrand, T.G., 1978, Preliminary documentation of program "FFTFIL", U.S. Geological Survey, Denver.

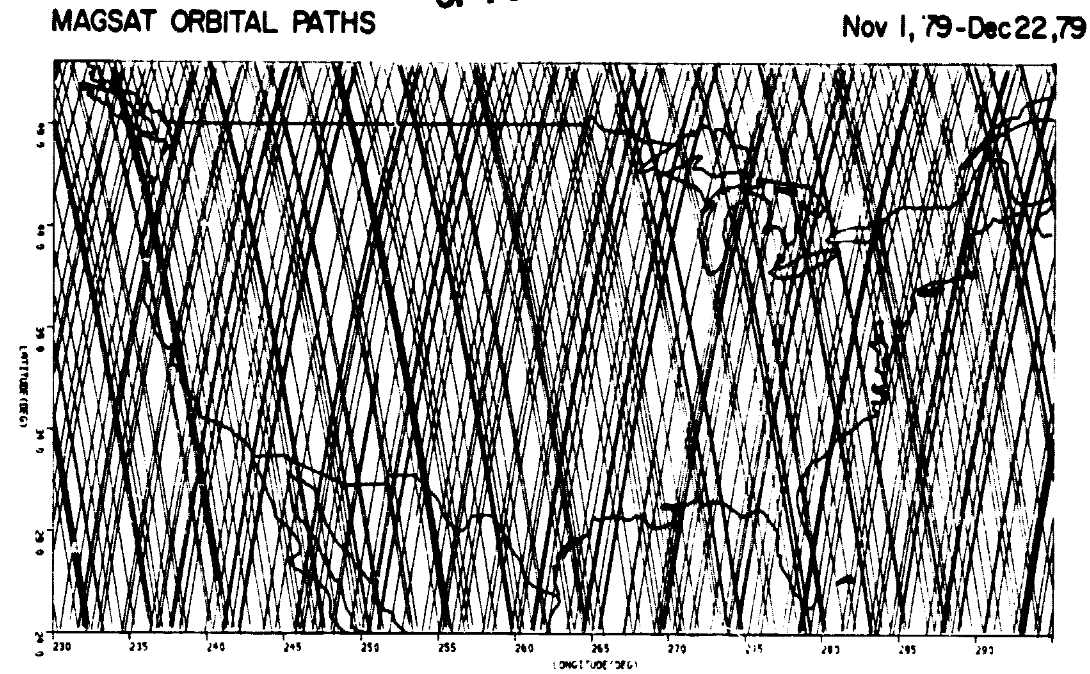

Figure 1. MAGSAT orbital paths over the U.S. between November 1, 1979 and December 22, 1979. Counting the north-bound and the south-bound paths separately, there are a total of 306 paths in the area.

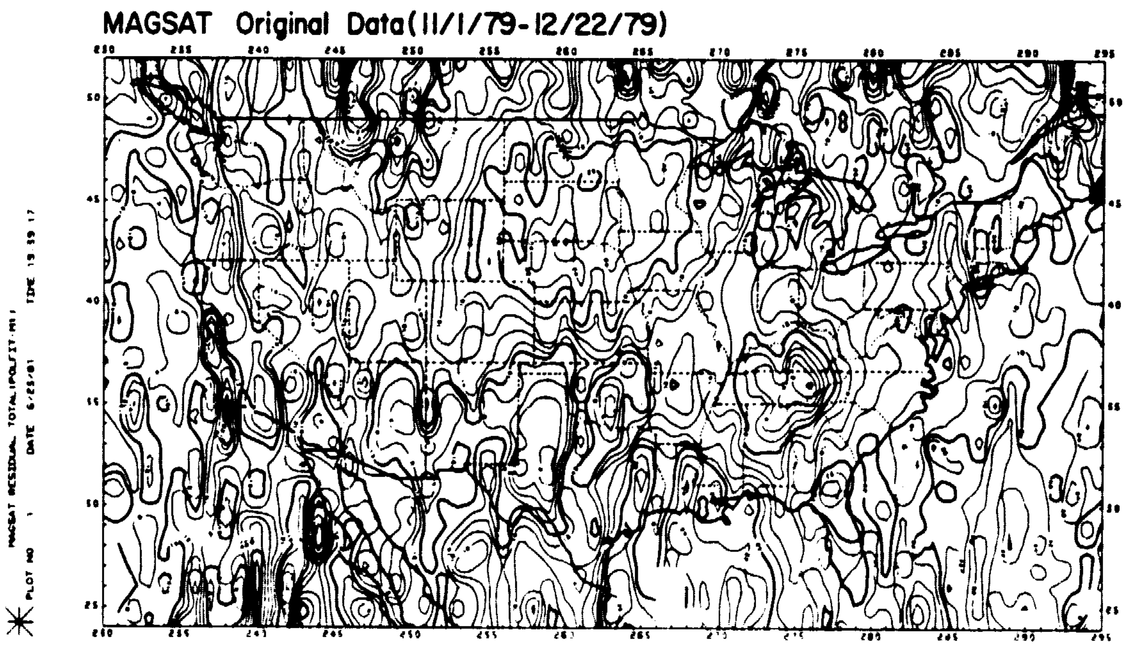

Figure 2. MAGSAT scalar anomaly map using the original data along 306 paths shown in Figure 1. Contour interval: 2 gammas.

ORIGINAL PAGE IS
OF POOR QUALITY

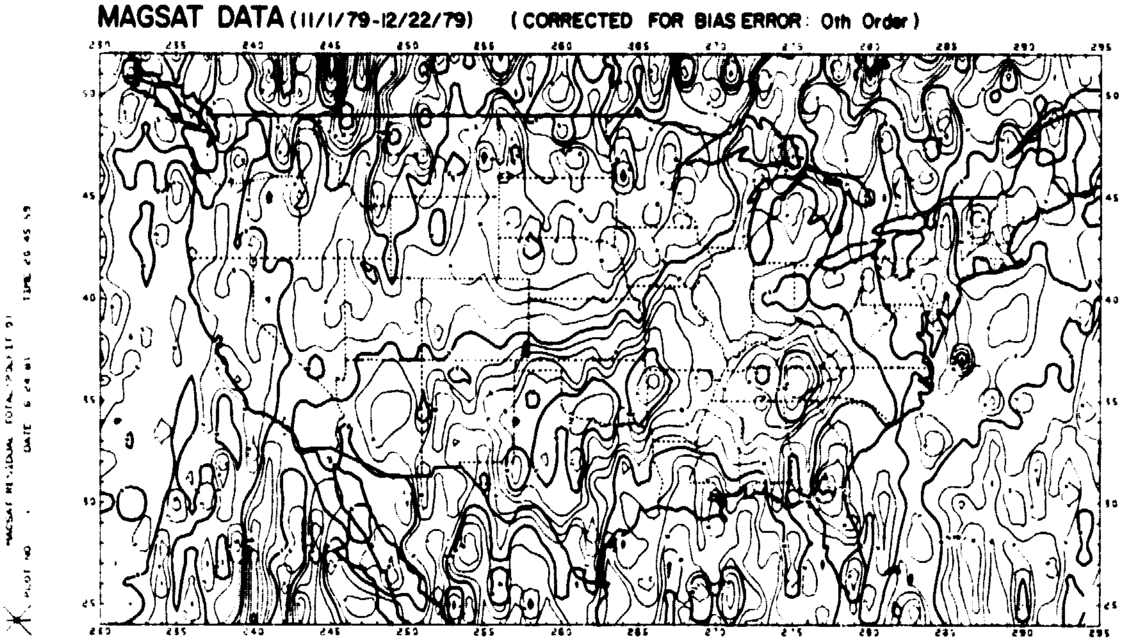

Figure 3. MAGSAT scalar anomaly map after removing the orbital static bias error from each data path. Contour interval: 2 gammas.

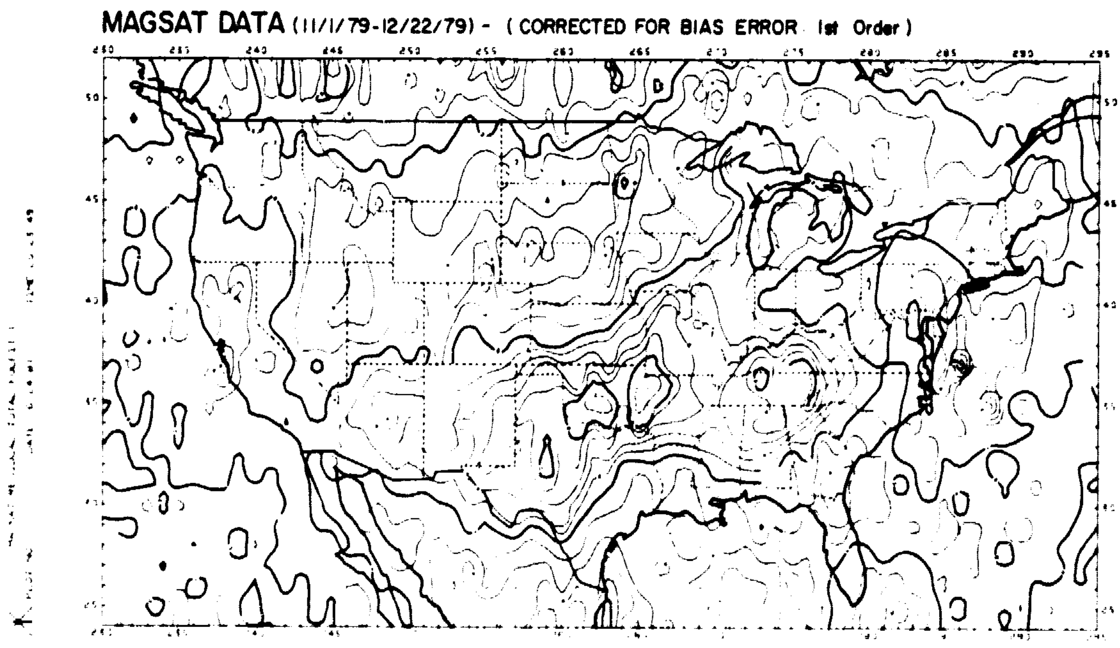

Figure 4. MAGSAT scalar anomaly map after removing the static bias and drift from each data path. Contour interval: 2 gammas.

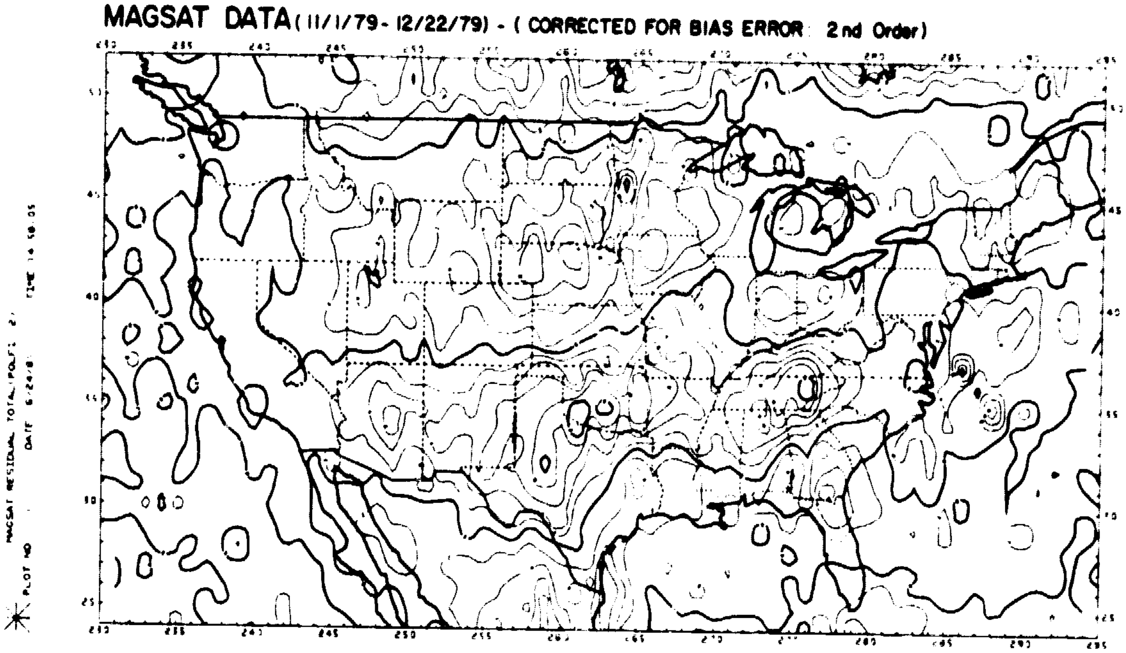

Figure 5. MAGSAT scalar anomaly map after removing a second-order polynomial from each data path. Contour interval: 2 gammas.

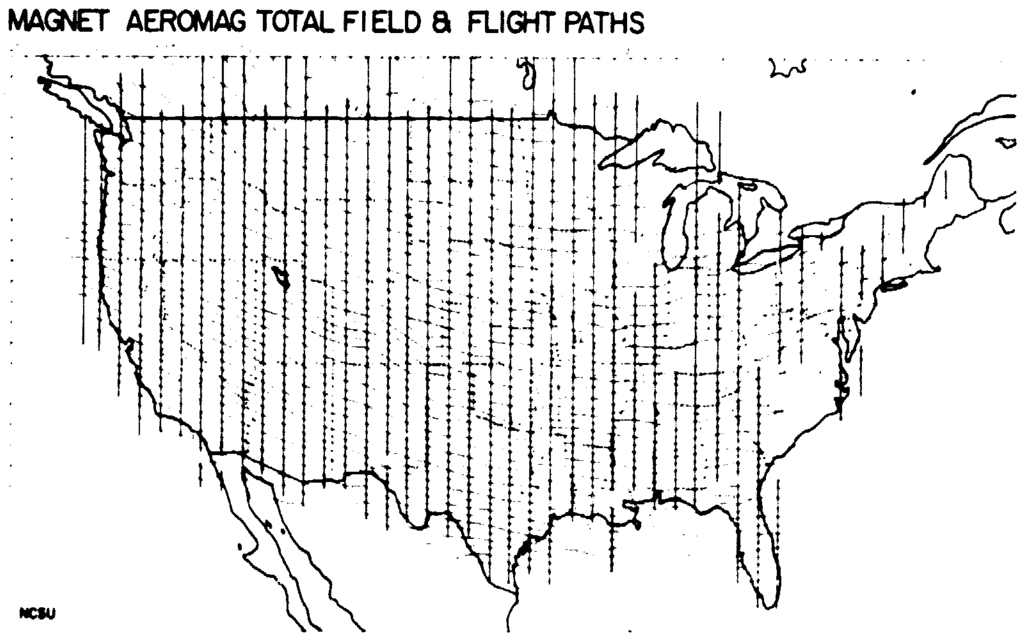

Figure 6. MAGNET flight paths and the total field map. Contour interval: 250 gammas.

ORIGINAL PAGE IS
OF POOR QUALITY

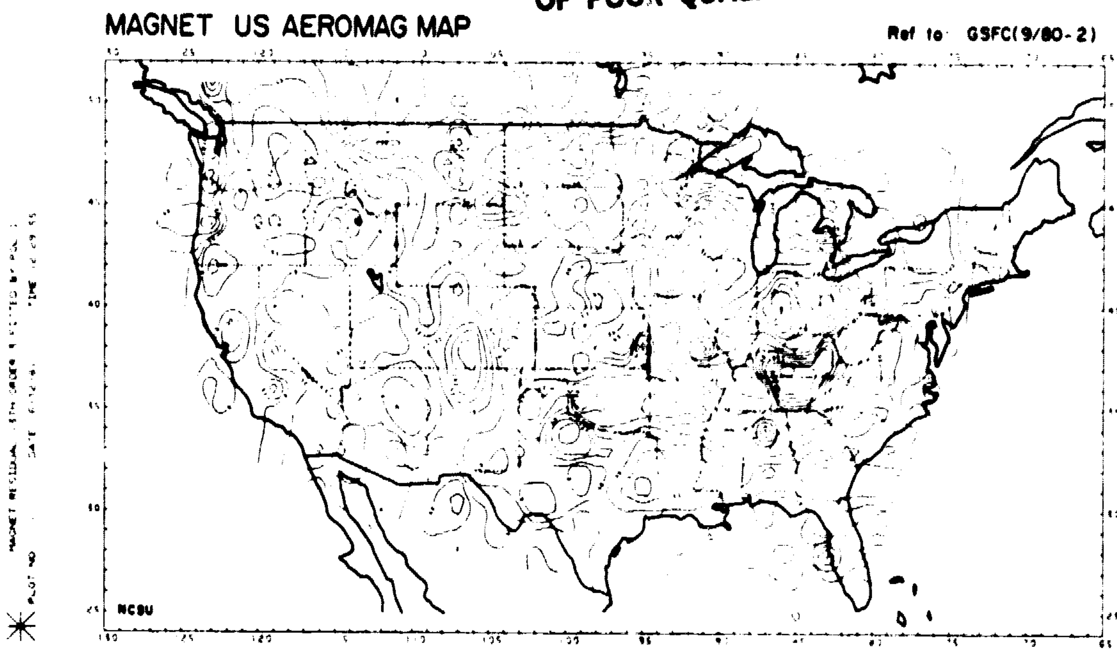

Figure 7. MAGNET U.S. Aeromagnetic map referenced to the GSFC (9/80-2) field model. Contour interval: 50 gammas.

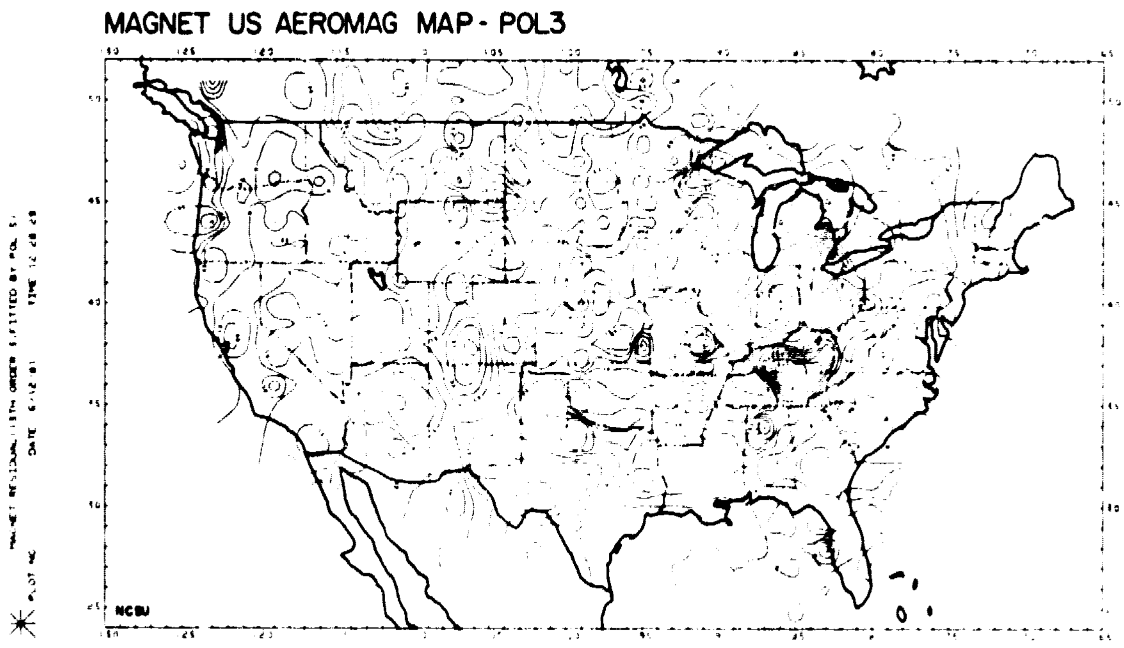

Figure 8. MAGNET U.S. Aeromagnetic map referenced to the GSFC (9/80-2) field model after removing a best-fit third order polynomial surface. Contour interval: 50 gammas.

ORIGINAL PAGE IS
OF POOR QUALITY

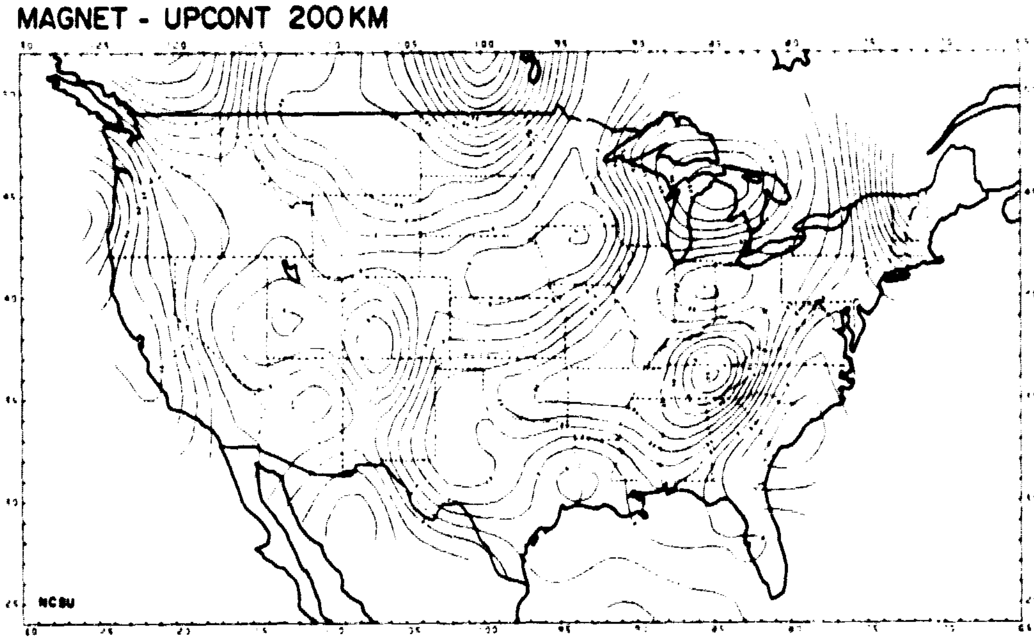

Figure 9. The MAGNET Aeromagnetic map of Figure 8 upward-continued to a 200 km altitude. Contour interval: 5 gammas.

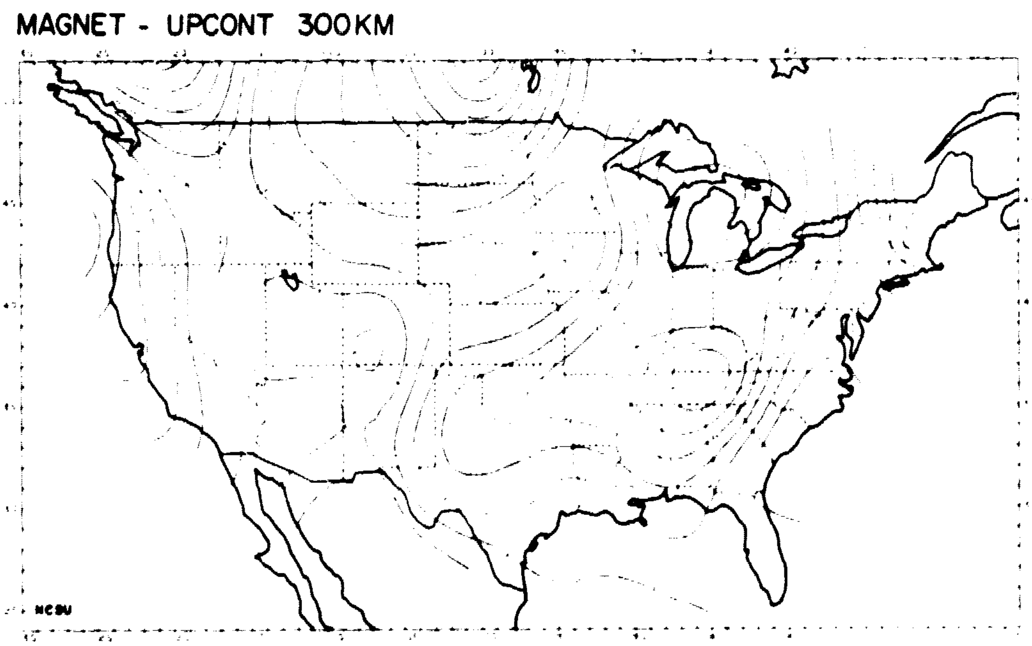

Figure 10. The MAGNET Aeromagnetic map of Figure 9 upward-continued to a 300 km altitude. Contour interal: 5 gammas.

ORIGINAL PAGE IS
OF POOR QUALITY

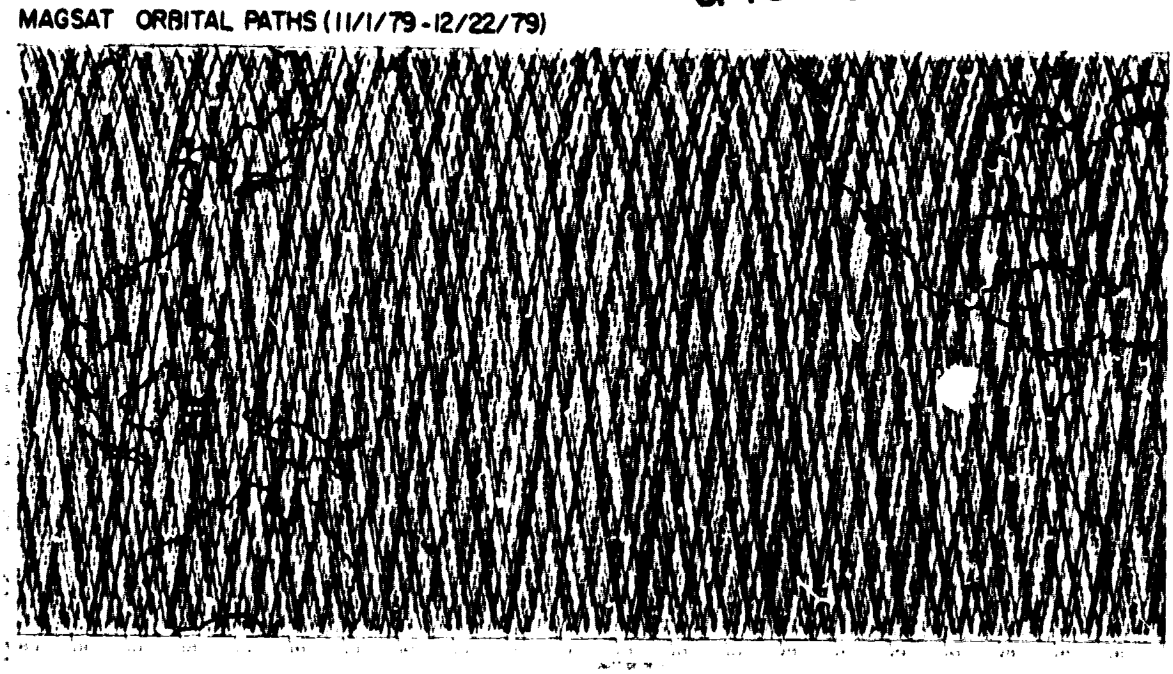

Figure 11. MAGSAT orbital paths over the Pacific region between November 1, 1979 and December 22, 1979. Counting the north-bound and the south-bound paths separately there are a total of 943 paths in the area.

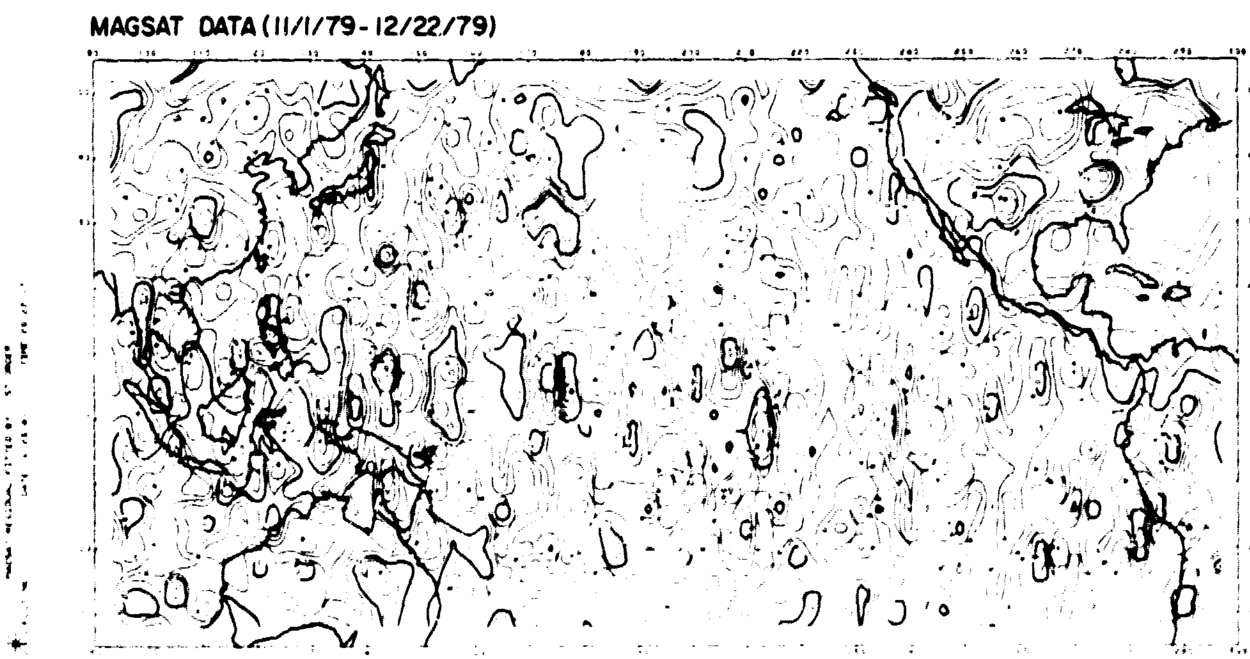

Figure 12. MAGSAT scalar anomaly map using the original data of 943 paths shown in Figure 11. Contour interval: 2 gammas.

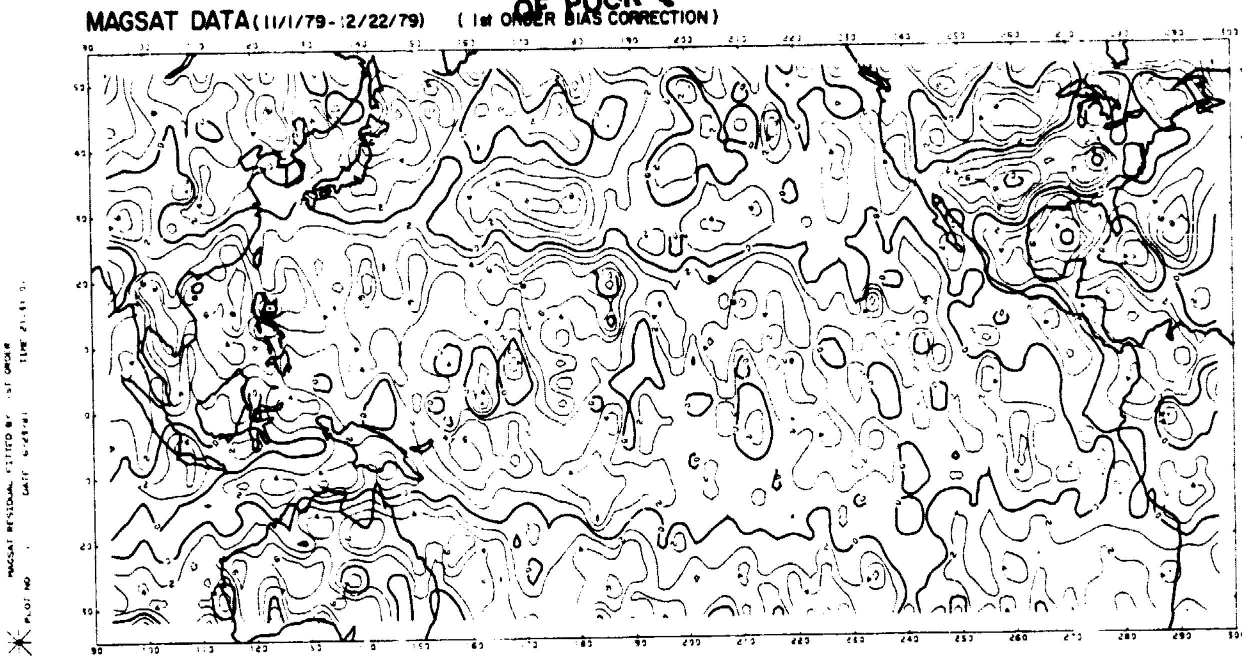

Figure 13. MAGSAT scalar anomaly map after removing a best-fit first order polynomial from each path. Contour interval: 2 gammas.

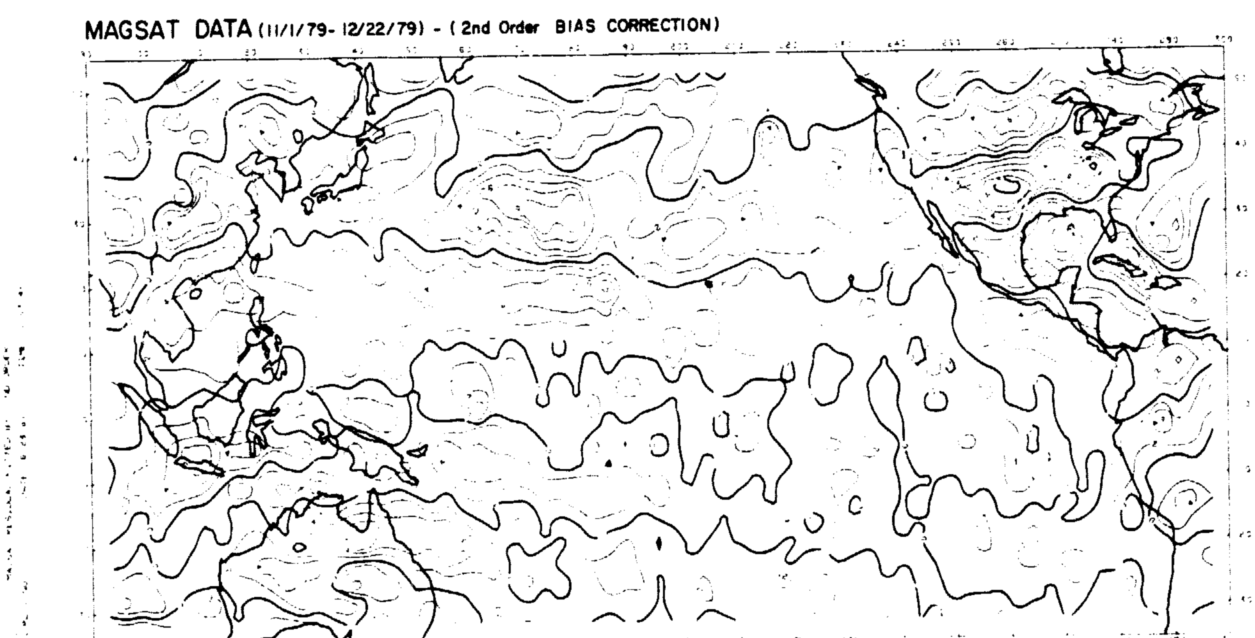

Figure 14. MAGSAT scalar anomaly map after removing a best-fit second-order polynomial from each path. Contour interval: 2 gammas.

ORIGINAL PAGE IS
OF POOR QUALITY

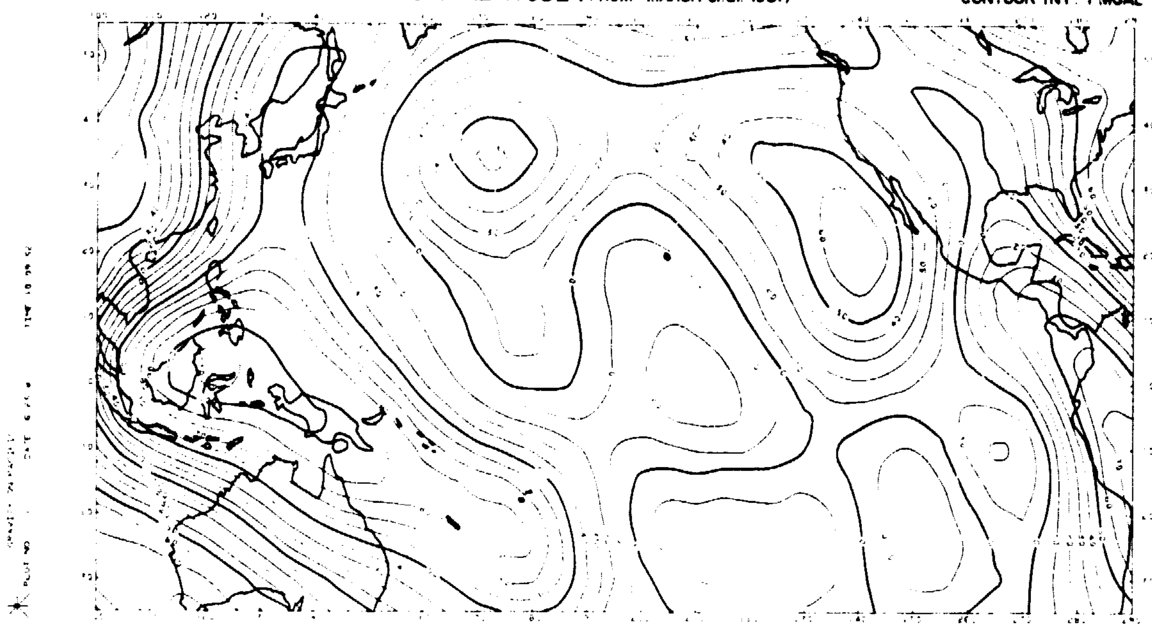

Figure 15. Gravity anomaly at GEOS-3 altitude derived from satellite to satellite tracking data. Contour interval: 1 mgal. (from Marsh, et al., 1981).

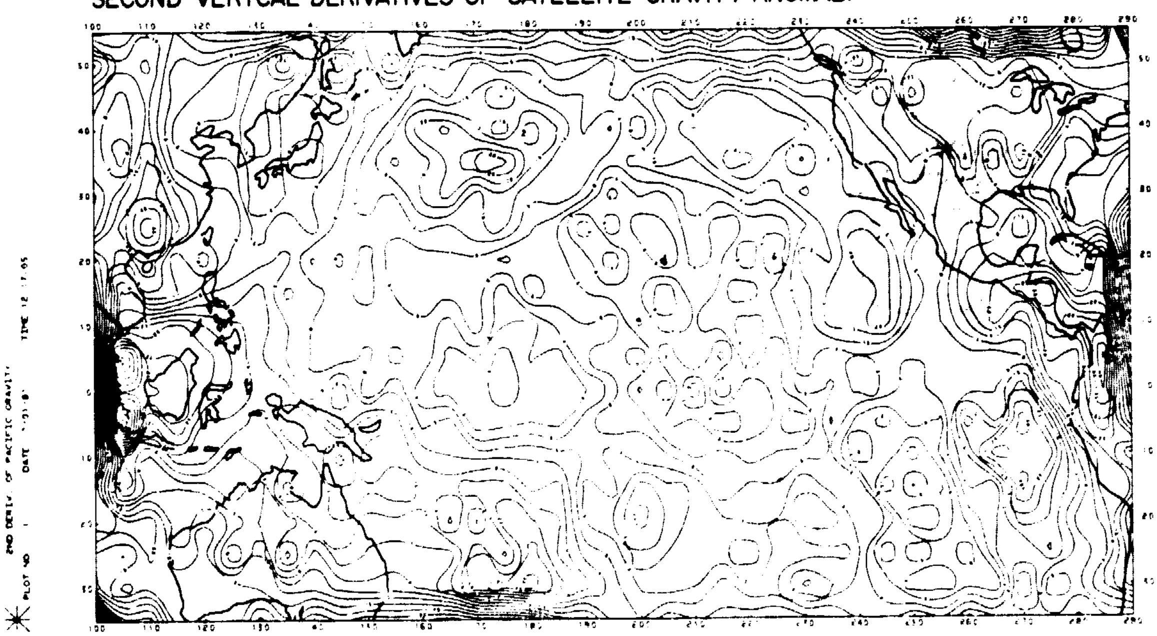

Figure 16. Second vertical derivative map derived from the gravity anomaly of Figure 15. Contour interval: $2x10^{-5}$ mgal/km/km.